Published in final edited form as:
Magn Reson Med. 2008 October ; 60(4): 970–975. doi:10.1002/mrm.21678.

Four-Dimensional Transcatheter Intra-arterial Perfusion (TRIP)-MRI for Monitoring Liver Tumor Embolization in VX2 Rabbits

Dingxin Wang, MS[1,2], **Sumeet Virmani, MD**[1], **Richard Tang, MD**[1], **Barbara Szolc-Kowalska, MD**[3], **Gayle Woloschak, PhD**[3,4], **Reed A. Omary, MD, MS**[1,2,4], and **Andrew C. Larson, PhD**[1,2,4]

[1] Department of Radiology, Northwestern University, Chicago, IL, USA

[2] Department of Biomedical Engineering, Northwestern University, Chicago, IL, USA

[3] Department of Radiation Oncology, Northwestern University, Chicago, IL, USA

[4] Feinberg School of Medicine, Robert H. Lurie Comprehensive Cancer Center, Northwestern University, Chicago, IL, USA

Abstract

TRanscatheter **I**ntraarterial **P**erfusion (TRIP)-MRI is an intra-procedural technique to iteratively monitor liver tumor perfusion changes during transcatheter arterial embolization (TAE) and chemoembolization (TACE). However, previous TRIP-MRI approaches using 2D T1-weighted saturation-recovery GRE sequences provided only limited spatial coverage and limited capacity for accurate perfusion quantification. In this pre-clinical study, a quantitative four-dimensional (4D) TRIP-MRI technique (serial iterative 3D volumetric perfusion imaging) with rigorous radiofrequency B_1 field calibration and dynamic tissue longitudinal relaxation rate R_1 measurement is presented for monitoring intra-procedural liver tumor perfusion during TAE. 4D TRIP-MRI and TAE were performed in 5 rabbits with 8 VX2 liver tumors (N=8). After B_1 calibrated baseline and dynamic R_1 quantification, subsequent tissue contrast agent concentration time curves were derived. Single-input flow-limited pharmacokinetic model and peak gradient method were applied for perfusion analysis. Perfusion Fρ reduced significantly from pre-TAE 0.477 (95% CI: 0.384–0.570) to post-TAE 0.131 (95% CI: 0.080–0.183) (mL/min/mL, $p<0.001$).

Keywords

Transcatheter; Intraarterial; Iterative Perfusion; TAE; Liver tumor

INTRODUCTION

Minimally invasive catheter-directed therapies, such as transcatheter arterial embolization (TAE) and chemoembolization (TACE) are palliative treatments for liver cancer (1). Preferentially delivering embolic agents via catheters positioned within the hepatic arteries, TAE and TACE selectively reduce blood flow to the targeted tumors. These procedures are currently performed using x-ray digital subtraction angiography (DSA) guidance to estimate blood flow reductions (termed ‘embolization endpoints’) after each injection of embolic materials. However, DSA flow estimates may be highly subjective and poorly reflect tumor perfusion (2). These potential limitations are particularly problematic because under-

The corresponding author: Andrew C. Larson, Ph.D., Northwestern University, Department of Radiology, 737 N. Michigan Avenue, Suite 1600, Chicago, IL 60611, Tel: (312) 926-3499, Fax: (312)926-5991, a-larson@northwestern.edu.

embolization may reduce therapeutic efficacy while over-embolization may harm adjacent uninvolved liver tissue.

TRanscatheter **I**ntraarterial **P**erfusion (TRIP) MRI is a recently developed intra-procedural technique to objectively monitor tumor perfusion changes during catheter-directed embolotherapies (2–5). TRIP-MRI uses targeted intraarterial (IA) gadolinium-based contrast injections through a selectively positioned catheter. Targeted delivery of contrast agent greatly conserves contrast dose, shortens requisite contrast wash-out time (6), and consequently permits serial iterative TRIP-MRI tumor perfusion measurements during therapy (3). Furthermore, for liver tumor perfusion measurements the targeted delivery of contrast agent to the hepatic artery simplifies pharmacokinetic analysis by requiring the consideration of only a single arterial input supply (3). Additionally, targeted IA contrast delivery allows a controllable pattern of contrast bolus injection which should benefit quantitative perfusion analysis.

TRIP-MRI monitoring can detect intra-procedural reductions to tumor perfusion during TAE in rabbit liver tumors (3) and during TACE in patients with hepatocellular carcinoma (HCC) (2,5). With TRIP-MRI feedback, interventional radiologists may be able to target specific embolic endpoints. However, previous TRIP-MRI approaches using 2D T1-weighted saturation-recovery spoiled gradient recall echo (GRE) sequences (2,3,5) offered limited spatial coverage and relatively poor signal-to-noise ratio (SNR). Furthermore, by simply assuming a linear correlation between image signal intensity and tissue contrast concentration, the quantitative accuracy of these approaches during iterative perfusion measurements remained limited. In this pre-clinical study, we present a quantitative four-dimensional (4D) TRIP-MRI technique (serial iterative three-dimensional volumetric perfusion imaging) with rigorous radiofrequency B_1 field calibration and dynamic tissue longitudinal relaxation rate R_1 measurement for intra-procedural assessment of liver tumor perfusion reductions during TAE.

METHODS

Animal Model

Our institutional Animal Care and Use Committee approved all experiments. Five New Zealand white rabbits (Covance, Denver, Pa) weighing 4–5 kg were used in these experiments. The rabbit VX2 tumor model was used because the VX2 tumor blood supply is similar to that of human HCC and rabbit hepatic arteries are sufficiently large to permit hepatic artery catheterization (3). VX2 cells were initially grown in the hindlimb of a donor rabbit. Tumor chunks approximately 2–3 mm in diameter were harvested and implanted in the left liver lobe of the rabbits during mini-laparotomy procedure. In five rabbits, eight VX2 liver tumors were grown. Liver tumors were incubated for 3 weeks prior to imaging.

X-ray DSA

DSA using a Siemens C-arm PowerMobil unit (Siemens Medical Solutions, Erlangen Germany) guided hepatic artery catheterization. Each rabbit was initially sedated using a mixture of IM ketamine (80 mg/kg) and xylazine (5 mg/kg). After intubation, inhalational isoflurane (2–3.5%) was administered for anesthesia through an endotracheal tube with a small animal ventilator. Via femoral artery access, a 2-F catheter (JB-1, Cook, Bloomington, IN) was advanced super-selectively over a 0.014-inch-diameter guide wire into the left hepatic artery that supplied the targeted tumor. DSA of the hepatic arteries was performed using 2 mL manual injections of iodinated contrast agent (iohexol, Omnipaque 350; Amersham, Princeton, NJ). The catheter was secured in its selected position with a 2-0 silk suture in the rabbit's groin. Each animal was then transferred to an adjacent MR scanner. All

subsequent TRIP-MRI scans and TAE procedures were performed with rabbits positioned inside the MR scanner.

MR Imaging

MR imaging was performed before and immediately after TAE using a 1.5T Magnetom Sonata clinical MRI scanner (Siemens Medical Solutions, Erlangen, Germany). Rabbits were imaged in the supine position using a clinical head coil. To avoid registration complications, rabbits remained within the scanner bore throughout TRIP-MRI and TAE procedures.

To depict tumor anatomy, 2D turbo spin-echo (TSE) T2-weighted images with full spatial coverage of the entire liver were first acquired with TR/TE = 3000/82 ms, 130 Hz/pixel BW, flip angle (FA) = 90°, 256×144 matrix, 5 mm slice thickness, 8 slices, 220×124 mm^2 FOV. To perform quantitative tumor perfusion imaging, an *in vivo* 3D B_1 map co-registered to the T2-weighted images was generated using a 3D multi-slab TSE double-angle method (DAM) with the following parameters: TR/TE = 6000/10 ms, 186 Hz/pixel BW, excitation/refocusing FA = 120°/120° and 60°/120°, respiratory belt triggered, multi-slab acquisition, 2 interleaved groups of slabs, 100% spacing, 100% slice oversampling, 220×124×40 mm^3 FOV, 128×72×8 matrix. Prior to each TRIP-MRI measurement, a baseline 3D R_{10} map co-registered to the B_1 map was acquired using 3D variable flip angle (VFA) spoiled-GRE method with the following parameters: TR/TE = 6/1.66 ms, 850 Hz/pixel BW, 50% slice over sampling, FA = 2°, 9°, 19°(7), 4 averages, 220×124×40 mm^3 FOV, 128×72×8 matrix. Slice oversampling was applied to avoid spatial wrapping of the RF transition region and side lobes. Eight vials with different concentrations of gadolinium contrast medium were placed next to each rabbit for R_{10} map calibration (8).

4D TRIP-MRI scans were performed with manual IA injections of 6.0 mL of a 1.25% gadopentetate dimeglumine solution (Gd-DTPA, Magnevist, Berlex, Wayne, NJ) over 10 sec using 3D GRE sequence (identical parameters to VFA sequence above) at 9° FA for rapid dynamic R_1 mapping following contrast injection. For each TRIP-MRI, the entire eight-partition volume of the liver was continuously sampled at 1.6-second intervals for 100 seconds. After TRIP-MRI, static 2D contrast-enhanced T1-weighted GRE images co-registered to the T2-weighted images were obtained with following parameters: TR/TE = 193/1.99 msec, 2 averages, FA = 80°, 480 Hz/pixel BW, 256×144 matrix, 5 mm slice thickness, 8 slices, 220×124 mm^2 FOV.

TAE

Embosphere® particles (BioSphere MedicalTM, Rockland MA) 40–120 μm in diameter were used as the embolic agent. TAE was performed 15 minutes after the first TRIP-MRI scan. No imaging guidance was used during the actual injection of Embospheres. However, each injection of Embospheres was performed with rabbits positioned inside the MR scanner bore. Embospheres® were super-selectively delivered by hand injection through the same same DSA catheter used for IA contrast injections. For each TAE, ~1.5 million microspheres were injected. Based upon results from a previous study (3), this embolic agent dose was chosen to reduce, but not eliminate antegrade blood flow to the tumor. After TAE and TRIP-MRI, rabbits were returned to DSA for follow-up angiography and confirmation of reduction to antegrade blood flow to the liver tumors. Each animal was then euthanized for tumor confirmation at gross necropsy.

MR Data Analysis

MR images were exported and processed with MATLAB software (Mathworks, Natick, MA).

B_1 calibrated baseline and dynamic R_1-mapping

The ratio between two DAM images at 120° and 60° FA was used to calculate the overall B_1 distribution, i.e. FA correction factor map (C_{FA}) (9):

$$C_{FA}(r)=\arccos(SI_{120}(r)/2SI_{60}(r))/60 \quad (1)$$

$C_{FA}(r)$ was used to correct the nominal excitation FA (α_{nom}) to actual FA value (α): $\alpha(r) = \alpha_{nom} \times C_{FA}(r)$. VFA spoiled-GRE steady-state signal intensities acquired at nominal 2°, 9°, and 19° FA were fit using B_1 calibrated integral signal equations over the image slice to calculate baseline 3D maps of longitudinal relaxation rate (R_{10}):

$$SI(r,\alpha_i)=M_0(r)\int_{slice}\sin(C_{FA}(r)\alpha_i(z))\frac{(1-E_{10}(r))}{(1-E_{10}(r)\cos(C_{FA}(r)\alpha_i(z)))}dz \quad (2)$$

where $E_{10}(r) = \exp(-TR \times R_{10}(r))$ and $M_0(r)$ is a constant associated with equilibrium magnetization and receiver coil gain. Nominal FA slice profiles were provided by numerically solving Bloch equations based upon pulse sequence RF definitions.

After deriving 3D R_{10} maps, the signal ratios between TRIP-MRI dynamic and baseline spoiled-GRE images both at 9° FA were fit using B_1 calibrated integrated steady-state signal equation to generate the time series of 3D maps of longitudinal relaxation rate $R_1(t)$:

$$\frac{SI_d(r,t,\alpha_9)}{SI(r,\alpha_9)}=\frac{\int_{slice}\sin(C_{FA}(r)\alpha_9(z))\frac{(1-E_1(r,t))}{(1-E_1(r,t)\cos(C_{FA}(r)\alpha_9(z)))}dz}{\int_{slice}\sin(C_{FA}(r)\alpha_9(z))\frac{(1-E_{10}(r))}{(1-E_{10}(r)\cos(C_{FA}(r)\alpha_9(z)))}dz} \quad (3)$$

where $E_1(r,t) = \exp(-TR \times R_1(r,t))$

Conversion of $R_1(t)$ - contrast agent concentration

Each voxel within the 3D volume $R_1(t)$ derived from each TRIP-MR image series was converted into a time series of tissue contrast agent concentration measurements using the classic relationship:

$$C_t(t)=[R_1(t)-R_{10}]/\Re_1 \quad (4)$$

with $\Re_1$ the longitudinal relaxivity of Gd-DTPA (3.9 $Ls^{-1}mmol^{-1}$ at 37°C) (10). This conversion assumes fast exchange of water protons between compartments and that Gd-DTPA relaxivity does not significantly differ between blood and extra-vascular space (11,12). The time series of 3D contrast agent concentration maps were used for quantitative perfusion analysis.

Perfusion analysis

With IA injection and flow-limited conditions common to tumor microvasculature, the rate of contrast tracer uptake in liver tumor is described using the single-input flow-limited pharmacokinetic model (13,14):

$$G_t(t)=dC_t(t)/dt=F\rho(C_a(t)-C_v(t)) \quad (5)$$

with $G_t(t)$ tissue contrast agent uptake gradient (mmol/mL/min), $C_t(t)$ tumor tissue, $C_a(t)$ arterial blood and $C_v(t)$ venous blood contrast agent concentrations (mmol/mL), F perfusion flow (mL/min/100g), ρ tissue density (100g/mL). Assuming $C_a(t) \gg C_v(t)$ during first pass of the contrast bolus (15), venous drain can be ignored, Equ. 5 can be simplified as

$$G_t(t)=F\rho C_a(t) \quad (6)$$

Therefore, perfusion maps $F\rho$ were calculated using peak gradient method (16,17):

$$F\rho=\max\{G_t(t)\}/\max\{C_a(t)\} \quad (7)$$

where $\max\{G_t(t)\}$is the peak tissue contrast agent uptake gradient and $\max\{C_a(t)\}$is the maximum contrast agent concentration in the feeding vessel. For transcatheter IA contrast injection, since the flow rate of the catheter injection easily surpasses that of the feeding artery, this injection is assumed to dominate the maximum vascular contrast agent concentration as $\max\{C_a(t)\} \approx [Gd]_{inject}$. Based upon the 6 mL 1.25% Gd solution injection, $[Gd]_{inject}$ was calculated (= 6.25 mmol/L). Separate regions-of-interest (ROIs) were drawn on perfusion maps in peripheral hypervascular regions to measure tumor perfusion avoiding the typical necrotic core of VX2 tumors (3). Two ROIs were drawn in each tumor.

Tumor perfusion change after TAE was calculated as the percent reduction from pre-TAE perfusion value. The perfusion parameter $F\rho$ (mL/min/mL) and perfusion reduction (%) were reported as means and 95% confidence intervals (CIs). Perfusion measurements before and after TAE were compared using paired t-tests with α=0.05. Statistical analysis was performed by using Origin software (version 7.0; OriginLab, Northampton, MA).

RESULTS

TRIP-MRI perfusion measurements were performed in eight liver tumors during TAE. Tumors measured 1.5 to 2.5 cm in diameter. T2-weighted images successfully depicted tumor position (Fig. 1). Corresponding pre-TAE contrast-enhanced T1-weighted images, peak ΔR_1 and Fρ maps all demonstrated the characteristic peripheral hypervascular rim of the VX2 tumors (Fig. 1). Tumor contrast agent uptake and perfusion were greatly reduced in the corresponding post-TAE ΔR_1 and Fρ maps. The $\Delta[Gd][t]$ curves for different tumor voxels from a representative rabbit are shown in Fig. 2. $\Delta[Gd][t]$ for each tumor voxel was altered by embolization. A total of 16 ROIs were drawn for the eight VX2 tumors. Tumor perfusion Fρ decreased significantly from pre-TAE 0.477 (95% CI: 0.384–0.570) to post-TAE 0.131 (95% CI: 0.080–0.183) (mL/min/mL, $p<0.001$). These results corresponded to a reduction in tumor perfusion Fρ of 75.2% (95% CI: 67.9%–82.5%) (Fig. 3).

DISCUSSION

We have developed a quantitative 4D TRIP MR imaging technique for intra-procedural monitoring of liver tumor embolization in VX2 rabbits. Even while using a very small contrast dose for each measurement (<0.01 mmol/kg for each injection), our 4D TRIP-MRI approach successfully detected significant reductions in tumor perfusion during TAE.

Our 4D TRIP-MRI technique is capable of providing serial three-dimensional volumetric perfusion measurements at progressive stages of embolization during catheter-directed interventional procedures. Gd-DTPA has a relatively short plasma distribution and

elimination half life, 0.2±0.13 hours and 1.6±0.13 hours, respectively. However, with conventional dose and intravenous (IV) injection, the number of iterative dynamic contrast-enhanced (DCE) MRI measurements during a time-constrained interventional procedure remains limited by the both cumulative dose and requisite washout times between injections. Although previously a low-dose IV Gd-DTPA injection has been used to estimate arterial input function (AIF) in dual-bolus cardiac MR perfusion imaging (18), CNR was too low for meaningful myocardial perfusion evaluation at a low IV dose ≤ 0.01 mmol/kg (19). Targeted transcatheter IA injection has been shown to increase liver tumor conspicuity, permit more than 90% reduction in contrast agent dose compared with full-dose (0.1 mmol/kg) IV injection, and shorten contrast wash-out time which should allow serial iterative TRIP-MRI perfusion measurements during therapy (3,6). During iterative DCE-MRI measurements, previous contrast injections will inevitably influence the current contrast agent uptake profile. These effects could be a confounding factor for conventional IV injection DCE-MRI analyses which assess a 5 to 8 minute time-course post-injection. However, for our TRIP-MRI technique, only first-pass contrast kinetics were used to derive flow information and therefore residual contrast was not expected to have as significant an impact upon successive measurement. Previous studies demonstrated that up to five first-pass TRIP-MRI measurements could be performed within a one hour TAE procedure period (3). For these closely spaced scan iterations, rigorous B_1 field-calibrated R_1 measurements should further account for the adverse effects from cumulative tissue contrast agent concentration thereby improving accuracy during successive quantification of contrast kinetics during serial TRIP–MRI.

The accuracy of B_1 field calibrated VFA R_1 measurements has been previously demonstrated (7,20). The single angle-point dynamic R_1 measurement with B_1 calibration was applied for AIF measurement in rabbit hind limb (21). In our study, not only in-plane B_1 non-uniformity, but also through-plane non-ideal slice profiles were corrected by integrating the signals along imaging slice and using 3D slice over-sampling. In a previous study with rigorous calibration of both slice profiles and B_1 inhomogeneities (8), the calibrated VFA technique demonstrated high stability, accuracy and precision for 3D baseline and dynamic T_1 measurements with the maximum mean T_1 error <3.6%, and the maximum mean standard deviation <3.7%. Although R_2* saturation effect can cause underestimation of tissue R_1 during dynamic imaging, only small peak contrast agent concentration changes were observed in tumor tissue for each TRIP-MRI injection, well below the 2.5 mmol/L R_2* sensitivity threshold (calculated assuming transverse relaxivity of Gd-DTPA: 5.3 $Ls^{-1}mmol^{-1}$ at 37°C (10), TE = 1.66 ms, and 2% saturation) and therefore R_2* saturation effects should have been minimal.

A quantitative single-input flow-limited pharmacokinetic model was chosen for perfusion analysis because a) transcatheter IA injection simplifies liver perfusion modeling from a complex dual-supply to a single vessel input supply system; and b) permeability is much higher than blood flow in liver tumors (13,14) justifying an assumption of flow-limited conditions. For our study, first-pass conditions $C_a(t) \gg C_v(t)$ were assumed for each TRIP-MRI injection, although residual contrast agent may adversely alter iterative first-pass measurements. However, by using a small dose for each TRIP-MRI study and 15 minute delays between contrast injections, residual tissue and blood pool contrast agent concentrations were minimal compared to the injected contrast agent concentration. Furthermore, our study demonstrated only a single passage of the contrast agent bolus. Lack of a second contrast agent passage should limit cumulative dose to the targeted tissues. Additionally, a small amount of residual tissue contrast agent is expected to contribute only minor differences to the contrast uptake during the first-pass, provided flow-limited conditions and assumption of identical diffusion forces (19). Another assumption for our study was that the transcatheter IA contrast injection would dominate the maximum vascular

input concentration necessary for utilization of the peak gradient method. This assumption remains plausible given that the injection flow rate through the catheter was much greater than that of the small feeding artery and the highly super-selective IA injection was localized and proximal to the tumor perfusion region.

This study has several limitations. The primary limitation was a lack of gold-standard reference measurements to validate absolute tumor perfusion changes during TAE. However, such evaluation was beyond the scope of this initial study which aimed to establish the feasibility of 4D perfusion imaging during TAE. Furthermore, iterative administration of fluorescent or radiolabelled microspheres, for the purpose of gold-standard hepatic perfusion measurements, would require additional invasive procedures, complicating an already relatively time-constrained experiment. Previous studies in the rabbit model have already demonstrated a significant correlation ($r = 0.72$, $p < 0.012$) between microsphere perfusion reductions and semi-quantitative TRIP-MRI area under the curve (AUC) measurements (4). Another limitation was that contrast agent dose with respect to targeted lobar and tumor volumes, frequency of iterative TRIP-MRI measurements, and contrast agent injection rate were not rigorously optimized in this study. TRIP-MRI contrast dose optimization will be an important objective for future studies. Finally, catheter placement within hepatic arteries may lead to transient intra-procedural obstructions to arterial flow and subsequent TRIP-MRI underestimation of the permanent post-procedural perfusion change following catheter withdrawal. Further studies are necessary to evaluate the impact of catheter-based flow obstructions in the setting of TRIP-MRI perfusion measurements. Nonetheless, even if TRIP-MRI were to systematically underestimate absolute perfusion values, these quantitative methods would still offer important improvements over highly subjective DSA approaches shown to have only moderate intra-observer agreement (Kappa statistic: $K = 0.46 \pm 0.12$) for monitoring embolic end-points during TACE procedures (2).

In conclusion, with intra-procedural B_1 field calibration and dynamic tissue R_1 measurement, quantitative 4D TRIP-MRI can monitor serial reductions in liver tumor perfusion during TAE in rabbits. Using hybrid MR-DSA units, future studies should aim to translate this technique clinically as a method to target objective embolic endpoints during TAE and TACE.

Acknowledgments

The authors thank Kathy R. Harris for expert assistance with animal model preparation and handling during TAE and MRI.

References

1. Llovet JM, Real MI, Montana X, Planas R, Coll S, Aponte J, Ayuso C, Sala M, Muchart J, Sola R, Rodes J, Bruix J. Arterial embolisation or chemoembolisation versus symptomatic treatment in patients with unresectable hepatocellular carcinoma: a randomised controlled trial. Lancet 2002;359(9319):1734–1739. [PubMed: 12049862]
2. Lewandowski RJ, Wang D, Gehl J, Atassi B, Ryu RK, Sato K, Nemcek AA Jr, Miller FH, Mulcahy MF, Kulik L, Larson AC, Salem R, Omary RA. A comparison of chemoembolization endpoints using angiographic versus transcatheter intraarterial perfusion/MR imaging monitoring. J Vasc Interv Radiol 2007;18(10):1249–1257. [PubMed: 17911515]
3. Wang D, Bangash AK, Rhee TK, Woloschak GE, Paunesku T, Salem R, Omary RA, Larson AC. Liver tumors: monitoring embolization in rabbits with VX2 tumors--transcatheter intraarterial first-pass perfusion MR imaging. Radiology 2007;245(1):130–139. [PubMed: 17885186]
4. Virmani S, Wang D, Harris KR, Ryu RK, Sato KT, Lewandowski RJ, Nemcek AA Jr, Szolc-Kowalska B, Woloschak G, Salem R, Larson AC, Omary RA. Comparison of transcatheter intraarterial perfusion MR imaging and fluorescent microsphere perfusion measurements during

transcatheter arterial embolization of rabbit liver tumors. J Vasc Interv Radiol 2007;18(10):1280–1286. [PubMed: 17911519]

5. Larson AC, Wang D, Atassi B, Sato KT, Ryu RK, Lewandowski RJ, Nemcek AA Jr, Mulcahy MF, Kulik LM, Miller FH, Salem R, Omary RA. Transcatheter intraarterial perfusion: MR monitoring of chemoembolization for hepatocellular carcinoma--feasibility of initial clinical translation. Radiology 2008;246(3):964–971. [PubMed: 18309018]
6. Larson AC, Rhee TK, Deng J, Wang D, Sato KT, Salem R, Paunesku T, Woloschak G, Mulcahy MF, Li D, Omary RA. Comparison between intravenous and intraarterial contrast injections for dynamic 3D MRI of liver tumors in the VX2 rabbit model. J Magn Reson Imaging 2006;24(1):242–247. [PubMed: 16758469]
7. Cheng HL, Wright GA. Rapid high-resolution T(1) mapping by variable flip angles: accurate and precise measurements in the presence of radiofrequency field inhomogeneity. Magn Reson Med 2006;55(3):566–574. [PubMed: 16450365]
8. Wang, D.; Virmani, S.; Koktzoglou, I.; Mulcahy, M.; Omary, R.; Larson, A. Rapid Dynamic 3D T1-Mapping of the Abdomen. Proceedings of the 15th Annual Meeting of ISMRM; Berlin, Germany. 2007. (Abstract 1792)
9. Stollberger R, Wach P. Imaging of the active B1 field in vivo. Magn Reson Med 1996;35(2):246–251. [PubMed: 8622590]
10. Pintaske J, Martirosian P, Graf H, Erb G, Lodemann KP, Claussen CD, Schick F. Relaxivity of Gadopentetate Dimeglumine (Magnevist), Gadobutrol (Gadovist), and Gadobenate Dimeglumine (MultiHance) in human blood plasma at 0.2, 1.5, and 3 Tesla. Invest Radiol 2006;41(3):213–221. [PubMed: 16481903]
11. Donahue KM, Weisskoff RM, Burstein D. Water diffusion and exchange as they influence contrast enhancement. J Magn Reson Imaging 1997;7(1):102–110. [PubMed: 9039599]
12. Judd RM, Reeder SB, May-Newman K. Effects of water exchange on the measurement of myocardial perfusion using paramagnetic contrast agents. Magn Reson Med 1999;41(2):334–342. [PubMed: 10080282]
13. Tofts PS, Brix G, Buckley DL, Evelhoch JL, Henderson E, Knopp MV, Larsson HB, Lee TY, Mayr NA, Parker GJ, Port RE, Taylor J, Weisskoff RM. Estimating kinetic parameters from dynamic contrast-enhanced T(1)-weighted MRI of a diffusable tracer: standardized quantities and symbols. J Magn Reson Imaging 1999;10(3):223–232. [PubMed: 10508281]
14. Collins DJ, Padhani AR. Dynamic magnetic resonance imaging of tumor perfusion. Approaches and biomedical challenges. IEEE Eng Med Biol Mag 2004;23(5):65–83. [PubMed: 15565801]
15. Jackson A, Haroon H, Zhu XP, Li KL, Thacker NA, Jayson G. Breath-hold perfusion and permeability mapping of hepatic malignancies using magnetic resonance imaging and a first-pass leakage profile model. NMR Biomed 2002;15(2):164–173. [PubMed: 11870912]
16. Bader TR, Herneth AM, Blaicher W, Steininger R, Muhlbacher F, Lechner G, Grabenwoger F. Hepatic perfusion after liver transplantation: noninvasive measurement with dynamic single-section CT. Radiology 1998;209(1):129–134. [PubMed: 9769823]
17. Kapanen MK, Halavaara JT, Hakkinen AM. Open four-compartment model in the measurement of liver perfusion. Academic radiology 2005;12(12):1542–1550. [PubMed: 16321743]
18. Kostler H, Ritter C, Lipp M, Beer M, Hahn D, Sandstede J. Prebolus quantitative MR heart perfusion imaging. Magn Reson Med 2004;52(2):296–299. [PubMed: 15282811]
19. Utz W, Niendorf T, Wassmuth R, Messroghli D, Dietz R, Schulz-Menger J. Contrast-dose relation in first-pass myocardial MR perfusion imaging. J Magn Reson Imaging 2007;25(6):1131–1135. [PubMed: 17520736]
20. Wang JH, Qiu ML, Kim H, Constable RT. T-1 measurements incorporating flip angle calibration and correction in vivo. Journal of Magnetic Resonance 2006;182(2):283–292. [PubMed: 16875852]
21. Cheng HL. T1 measurement of flowing blood and arterial input function determination for quantitative 3D T1-weighted DCE-MRI. J Magn Reson Imaging 2007;25(5):1073–1078. [PubMed: 17410576]

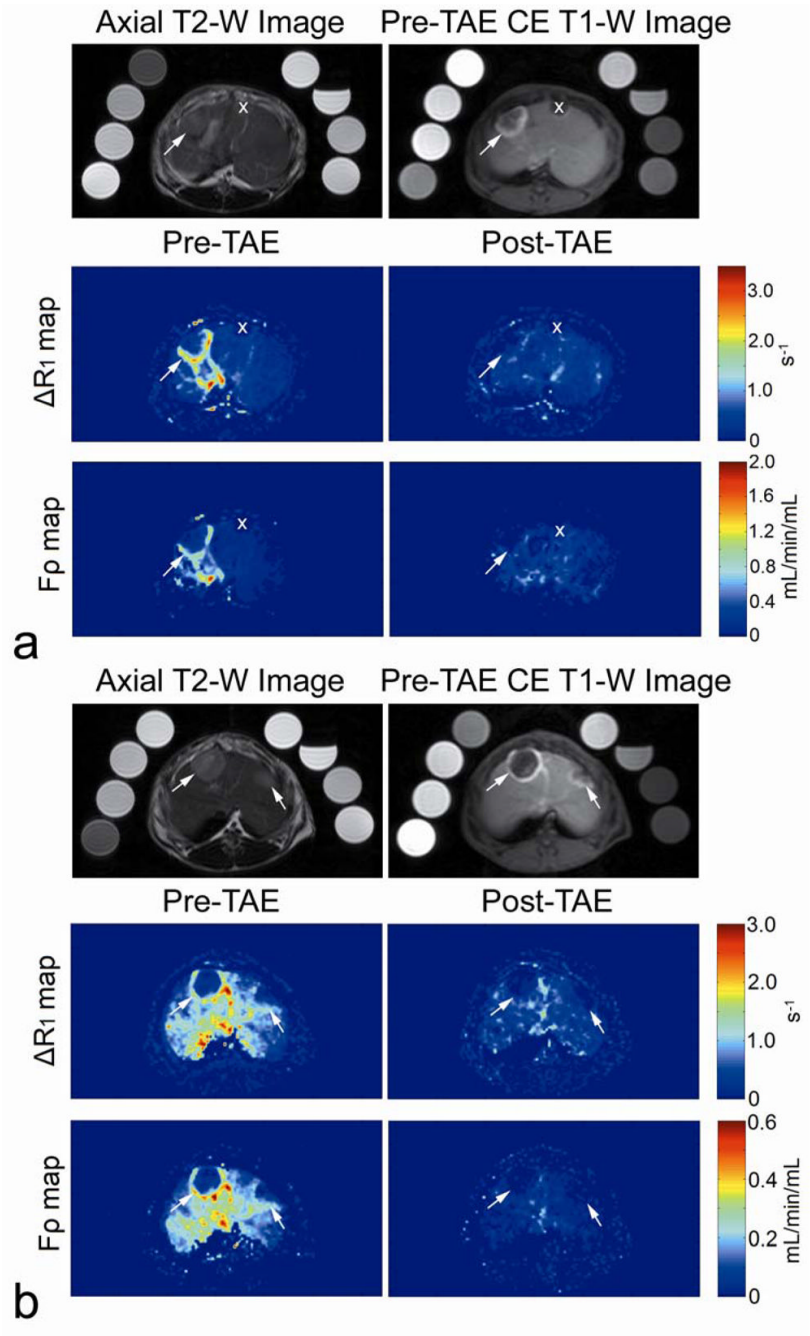

Figure 1.

Representative axial MR images in two VX2 liver tumor rabbits (a and b respectively). T2-weighted MR images (top left) show VX2 tumor position (arrows). Pre-embolization static contrast-enhanced T1-weighted MR images (top right), TRIP-MR peak ΔR1 (middle left) and perfusion Fρ (bottom left) maps demonstrate characteristic peripheral hypervascular rim in each VX2 tumor (arrows). Post-embolization TRIP-MR peak ΔR1 (middle right) and perfusion Fρ (bottom right) maps demonstrated reduced contrast agent uptake and perfusion of the tumors in the corresponding regions (arrows). The eight vials positioned around the rabbit were used for T1 calibration. Also notice that in upper rabbit (a) both TRIP-MR peak

ΔR1 and perfusion Fρ maps do not depict a small VX2 tumor (X), because this tumor was not located within the vascular territory targeted by IA injection.

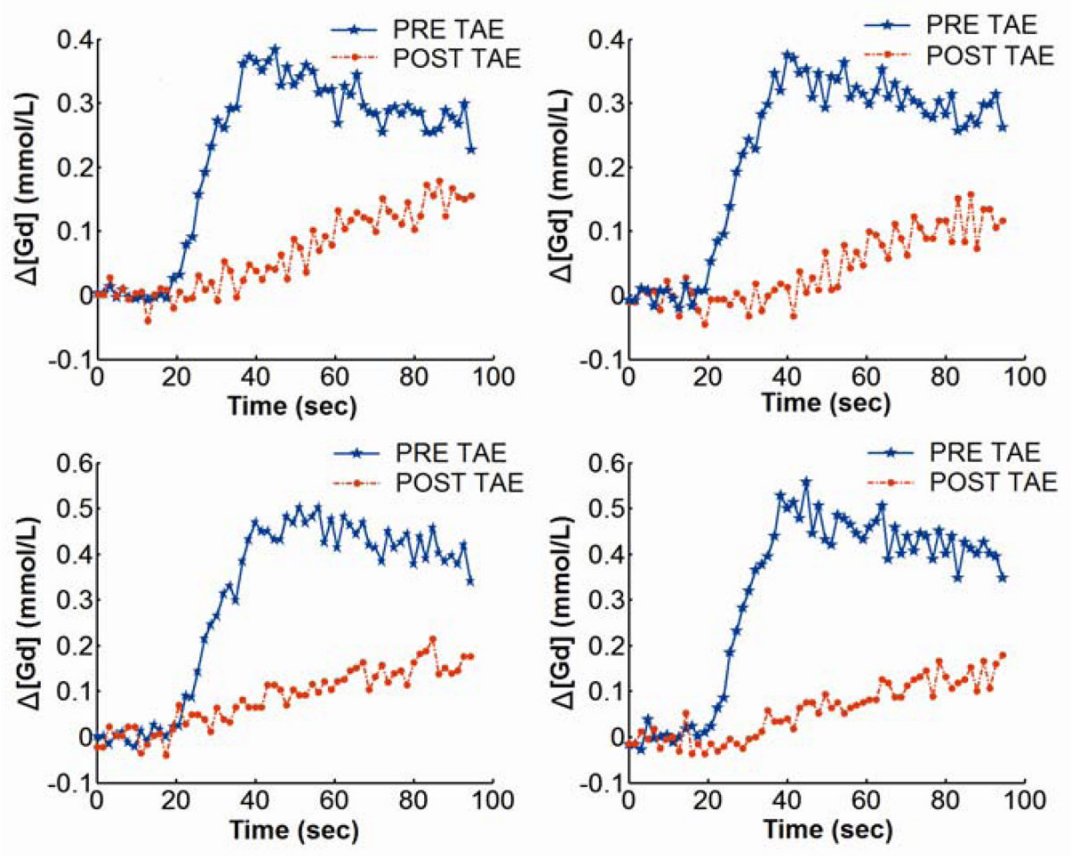

Figure 2.
Representative Δ[Gd](t) curves for 4 different voxels of a VX2 liver tumor rabbit before and after TAE. The Δ[Gd](t) curve altered in both shape and amplitude for each tumor voxel after TAE.

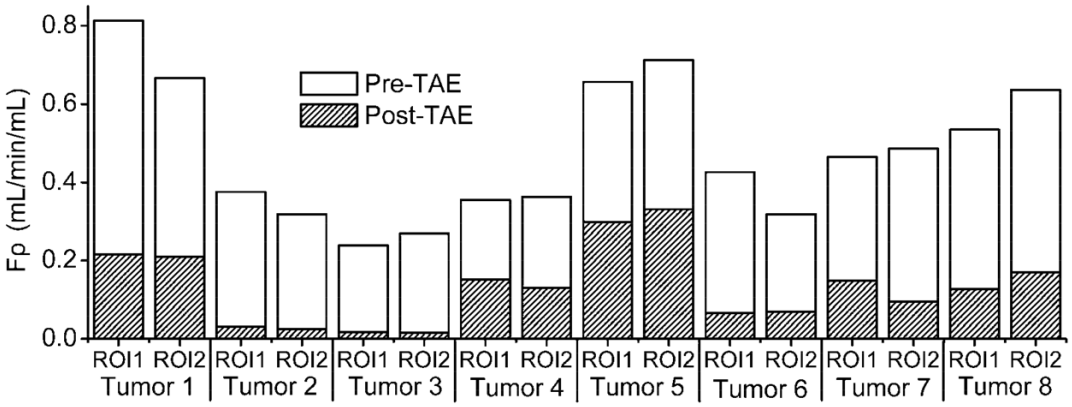

Figure 3.
Graph shows the reduction of quantitative tumor perfusion parameter Fρ after Embosphere® injection in each individual tumor ROI. ($p<0.001$)